

Design and simulation of low-loss Y-branch splitter with a channel profile of proton-exchanged lithium niobate

M. KAVOSH TEHRANI*, M. HAMI

Institute of Optics and Laser, Malek-Ashtar University of Technology, Shahin Shahr 83145/115, Iran

In this paper, an optimum single-mode optical coupler (power splitter) is simulated based on symmetric Y-branch comprising S-Bend Cosine waveguide with a channel profile of proton-exchanged lithium niobate. The distance between the two output waveguides is 127 μ m (center-to-center) which is suitable for the connection with the fibers. Since the angle of branches and their lengths affect the loss of Y-splitter, the simulations are performed for different angles and lengths. Optimum length for S-Bend Cosine waveguide is obtained and subsequently the loss of Y-splitter reaches the minimum value of 0.18 dB.

(Received October 31, 2016; accepted June 7, 2017)

Keywords: Waveguide, Optical coupler, Y-branch splitter, Proton-exchange, Lithium niobate, S-Bend Cosine

1. Introduction

Y-branch splitter are key components allowing confining and guiding light in optical integrated circuits (OIC). Lithium niobate (LiNbO₃, LN) is one of the most widely used materials for hosting OIC devices. LiNbO₃ is a synthetic dielectric material that does not exist in nature. Historically, it was first discovered in 1949 [1], but the growth as single crystals was achieved in 1965 [2]. It shows extremely high nonlinear optical coefficients [3], which makes it a favorite candidate for the realization of optical devices such as parametric oscillators, parametric amplifiers, second harmonic generators, modulators, etc.

Many techniques such as ion/metal diffusion (e.g. titanium diffusion [4,5] or the proton exchange [6]) and ion beam implantation [7] are used to fabricate waveguides in LiNbO₃. Waveguides made by Ti diffusion suffer from increased photorefractive damage, which means that the devices cannot operate at very high power densities in the visible [4]. Furthermore, high processing temperatures complicate the fabrication of waveguides. Ion beam implantation (IBI) is a process that changes the properties of a material by forcefully embedding different types of ions in it. It typically gives a negative index change in a buried region where the bombarding ions stop in the crystal. IBI is suitable for materials that can have major changes in their properties caused by a small number of implanted particles, typically N⁺, B⁺, He⁺ and Ne⁺ [8]. It was reported that the ion beam implantation can affect the surface properties negatively, e.g. by increasing the hardness and resistance to oxidation [4]. Proton exchange (PE) is one of the most popular methods to fabricate waveguides. It consists of an ion exchange process taking place at the crystal surface, where lithium ions in LiNbO₃ are substituted by protons (H⁺) coming from an acidic melt solution. In contrast with Ti:diffusion, which yields waveguides guiding all polarizations in LN,

PE waveguides can only guide light of extraordinary polarization, i.e. light polarized along the crystal optical axis. The proton exchange technique is cheap, and simple; and it implies processing at relatively low temperatures (~200°C). The proton exchange increases the extraordinary refractive index by about $\Delta n_e = 0.12$ [9,10], while it decreases the ordinary refractive index by about $\Delta n_o = -0.04$ [9]. This anisotropic index change allows to guide the transverse electric (TE) mode in x and y-cut substrates and the transverse magnetic (TM) mode in z-cut substrates. A Y-branch splitter is one type of PELN waveguide. It is a fundamental element in constructing photonic integrated circuits such as power splitters, Mach-Zehnder interferometers, and hybrid-integrated optical transceivers. The Y-branch structure has an excellent performance in a very wide wavelength range, which means the Y-branch waveguide splitter can be further integrated into a ratio-metric wavelength measurement system [4]. A conventional Y-branch structure consists of an input waveguide and two branching waveguides, as shown in Fig. 1. The two branches either can have the shapes of S-Bend Sine, S-Bend Cosine and S-Bend Arc, or can be straight waveguides with a certain branching angle. Y-junction is composed of a base single-mode waveguide connected to two single-mode branch waveguides. Previously, the conventional Y-branch was found to suffer severe radiation loss when the branching angle was larger than 2° [11]. To reduce the loss, the branching angle must be small, and the length of the splitter device must be extended. To date, several efforts have been made to overcome the loss problem, especially when the branching angle is large [12-16].

In this paper, an optimum single-mode optical power splitter is simulated based on symmetric Y-branch comprising of S-Bend Cosine waveguides with a channel profile of proton-exchanged lithium niobate. The separation of branches is considered 127 μ m. The

optimum length of S-Bend Cosine part is obtained in which the loss of Y-splitter reaches the minimum value of 0.18 dB.

2. Y-branch splitter with S-Bend Cosine sections

A Y-branch splitter includes two tapered waveguide sections (in input ports), two S-Bend Cosine waveguide sections and two tapered waveguide sections (in output ports) as shown in Figure 1. In a Y-junction 3-dB coupler [17], the outer branches are kept geometrically symmetric to launch an equal amount of light into each waveguide, evenly distributing the optical input power into the two output ports. Such a coupler exhibits a better response for a wide range of applied optical power. Y-branch splitters are principally independent of wavelength and polarization. However, to achieve this unique feature, the angle between the Y-junction waveguides should be very small, which may lead to a longer device length. The coupling function $K(z)$ of a Y-junction structure can be described in terms of its waveguide shaping as follows [18]:

$$K(z) = K_0 \exp[-\gamma_3 d(z)] \quad (1)$$

Where $d(z)$ is the spacing between the two waveguides at position z , while γ_3 and K_0 are the waveguide decay value and coupling constant, respectively.

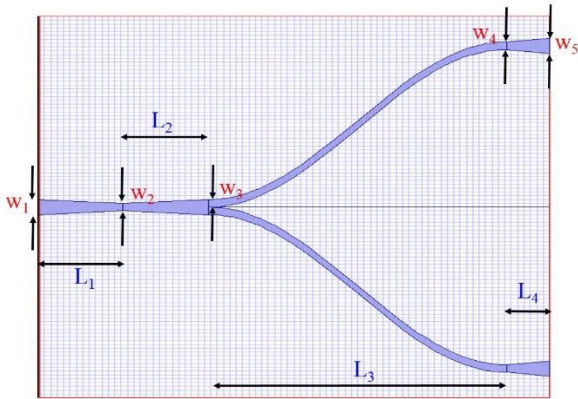


Fig. 1. Schematic of Y-branch splitter with S-Bend Cosine waveguides

Table 1. Device dimensions

w_1, w_5	$6\mu\text{m}$ (fixed)
w_2, w_3, w_4	$3\mu\text{m}$ (fixed)
L_1, L_2	$1000\mu\text{m}$ (fixed)
L_3	variable
L_4	$500\mu\text{m}$ (fixed)

Table 2. Design specifications

Wafer and guiding channel	
Device dimensions: Length with	Variable 0.15mm
Crystal cut direction	x-cut
Propagation direction	y
Substrate material (wafer)	LiNbO3
Cladding	air
Thickness: Cladding substrate	$10\mu\text{m}$ $100\mu\text{m}$
Proton-exchange process specifications	
Proton source	toluic acid
Process time	4h
Temperature	250 C
Diffusion constant [19]	$7.02 \times 10^7 \mu\text{m}^2\text{h}^{-1}$
Activation energy [19]	75.58kJmol^{-1}

The proposed structure of Y-branch splitter is based on a PE channel profile formed on an x-cut LN substrate. Proton exchange in LN replaces a few lithium ions by hydrogen ions (or protons) to make channel waveguides in LN substrate with a grade-function index profile. For our channel waveguide designs, toluic acid was applied as a source of hydrogen ions. Temperature and process time are considered $250\text{ }^\circ\text{C}$ and 4 hours, respectively.

Unfortunately, waveguides fabricated with pure melts have been found to be associated with serious problems, in particular, the degradation of the electrooptic coefficient, a large scattering and insertion loss, and refractive-index instabilities [20]. By using an annealing procedure, many of these problems can be avoided [20]. An accurate modeling of the PE index profile has presented using a Fermi function as well as the effects of various fabrication parameters on the propagation characteristics of single-mode APE waveguides [21]. According to [22], anneal temperatures (T_a) and times (t_a) ranged from $200\text{-}400\text{ }^\circ\text{C}$ and $0.25\text{-}16\text{ h}$, respectively. For fabrication of high quality waveguides (i.e., low loss, good electrooptic behavior, etc.), optimal anneal temperature is between $300\text{ }^\circ\text{C}$ and $360\text{ }^\circ\text{C}$ [22]. In our simulation, we consider anneal temperature of $360\text{ }^\circ\text{C}$ with time of 4 h.

According to Fig. 1, two tapered waveguide sections with a length of $1000\mu\text{m}$ for input ports and two tapered waveguide sections with a length of $500\mu\text{m}$ in each of output port have been chosen. These sections will have constant lengths in optimization process, and we only change the length of two S-Bend Cosine waveguides. The distance between the two output waveguides is $127\mu\text{m}$ (center-to-center). This value would not also be changed and is fixed. The initial and final widths of first tapered waveguide in the input port are considered 6 and $3\mu\text{m}$, respectively. The second tapered waveguide in the input port is opposite the first case i.e. 3 and $6\mu\text{m}$, respectively.

All dimensions of device and design specifications are listed in Tables 1 and 2. 2D and 3D refractive index distributions in XY plane are shown in Fig. 2(a) and 2(b). According to these Figures, the maximum difference of refractive index created by PE process is 0.048.

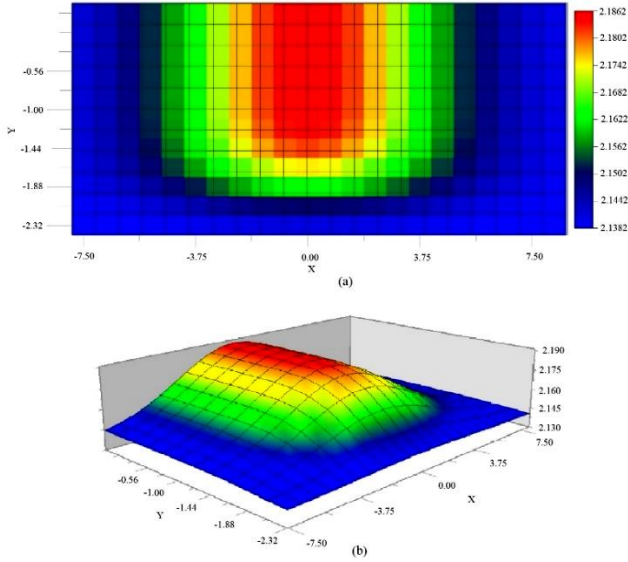


Fig. 2. Refractive index distribution in XY plane, 2D (a) and 3D (b)

3. Simulation and results

According to Tables 1 and 2, Y-branch splitter is designed by optiBPM software. Since the device is formed on an x-cut LN substrate, we analyzed its performance for TE-polarized optical inputs with a test wavelength of $1.55 \mu\text{m}$. We have evaluated the splitter in terms of the excess loss to obtain optimal design. The excess loss of the splitter is defined as [23]:

$$\text{excess loss} = -10 \log_{10} \left(\frac{P_{out}}{P_{in}} \right) \quad (2)$$

Where, P_{out} is total output power and P_{in} is the input power.

In our simulations, just one parameter is changed; that is, L_3 (the length of S-Bend Cosine waveguide section). The separation of output branches is fixed ($127 \mu\text{m}$) because of limitations in manufacturing and physical connections (also this value is suitable for coupling to optical fibers). Since we want to design a single-mode Y-

branch splitter, the widths of waveguides section are not changed. Therefore, simulations are performed for different values of L_3 ($1000, 1500, 3500, 7500, 11500$ and $15500 \mu\text{m}$), and then the optimal value is obtained. Fig. 3 shows the relative optical power as a function of propagation distance for different values of L_3 . It shows that the relative optical power decreases with the increase in propagation distance. According to Figure 3, the maximum relative power obtained at output ports is 0.96 at a wavelength of $1.55 \mu\text{m}$ (when the length of S-Bend Cosine waveguide is $3500 \mu\text{m}$; therefore, total length of device becomes $6000 \mu\text{m}$). This value is the total relative output power of two ports. According to equation (2), the excess loss of Y-splitter reaches a minimum value of 0.18 dB. After the successful simulation run by optiBPM software, we can view the refractive index profile and the electric field distribution in the simulation window. For optimum Y-branch splitter, the simulation results are shown in Figures 4 and 5. Figures 4(a) and 4(d) show 2D and 3D refractive index profiles in XZ plane, respectively. Figure 4(b) shows the refractive index profile in X-direction at $Z = 4200 \mu\text{m}$. The refractive index profile in Z-direction at $Y = -0.75 \mu\text{m}$ is shown in Figure 4(c). Fig. 4(a-d) show that how the refractive index profile change throughout the Y-branch splitter. 2D and 3D optical field distributions are presented in Figures 5(a) and 5(d), respectively. These results have been extracted at $Y = -1 \mu\text{m}$. Fig. 5(c) shows the optical field distribution in X-direction at $Z = 6000 \mu\text{m}$.

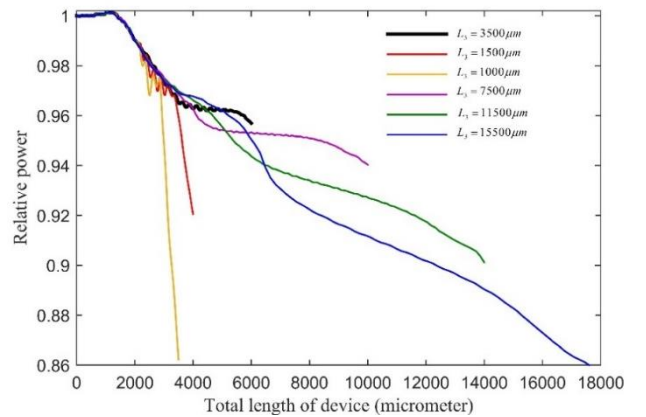


Fig. 3. Relative optical power as a function of propagation distance for different values of L_3

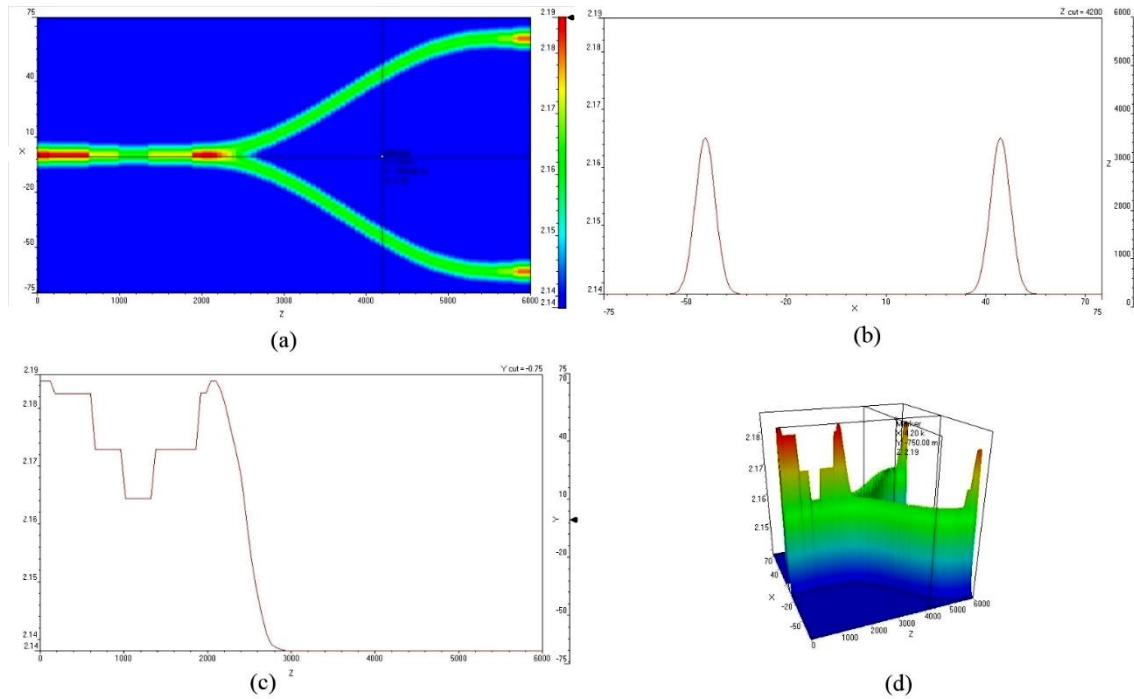


Fig. 4. Refractive index propagation in Y-branch splitter, (a) 2D refractive index profile in XZ plane, (b) the refractive index profile in X-direction at $Z = 4200\mu\text{m}$, (c) the refractive index profile in Z-direction at $Y = -0.75\mu\text{m}$, (d) 3D refractive index profile in XZ plane

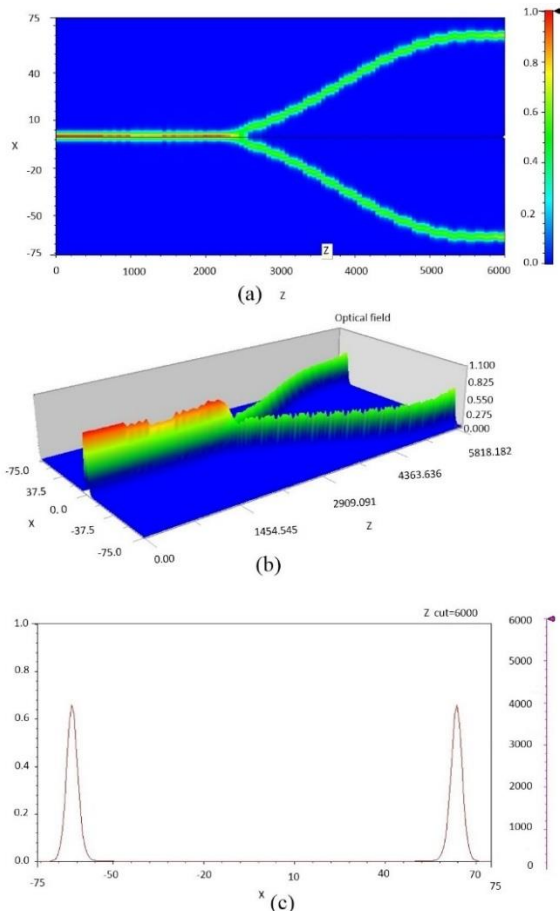


Fig. 5. (a) 2D and (b) 3D optical field distributions in XZ plane at $Y = -1\mu\text{m}$, (c) the optical field distribution in X-direction at $Z = 6000\mu\text{m}$

According to Fig. 5(a-c), it is clear that optical field distribution in output ports is symmetric and there is a minimum imbalance between two output ports.

4. Conclusion

In this paper, we managed to design and simulate an optimum single mode Y-junction beam splitter with a channel profile of proton-exchanged lithium niobate by optiBPM software. This Y-splitter has consisted of two tapered waveguide sections (in input ports), two S-Bend Cosine waveguide sections and two tapered waveguide sections (in output ports). For optimization, the width of waveguides and length of four tapered waveguides (in input and output ports) were considered fixed. We only changed the length of S-Bend Cosine waveguide. The minimizing loss was considered an optimization criterion. The excess loss of our optimum Y-branch splitter was 0.18 dB. This device can be used in Fiber-Optic Gyroscopes (FOGs).

References

- [1] B. T. Matthias, J. P. Rameika, Phys. Rev. **76**, 1886 (1949).
- [2] A. A. Ballman, J. Am. Ceram. Soc. **48**, 112 (1965).
- [3] R. S. Weis, T. K. Gaylord, Applied Physics A **37**, 191 (1985).
- [4] W. K. Burns, P. H. Klein, E. J. West, L. E. Plew, Journal of Applied Physics **50**, 6175 (1979).

- [5] W. S. Yang, H. -Y. Lee, W. K. Kim, D. H. Yoon, *Optical Materials* **27**, 1642 (2005).
- [6] J. L. Jackel, C. E. Rice, J. J. Veselka, *Appl. Phys. Lett.* **41**, 607 (1982).
- [7] P. D. Townsend, P. J. Chandler, L. Zhang, *Optical effect of ion implantation*, Cambridge University Press (1994).
- [8] Yu. N. Korkishko V. A. Fedorov, *Ion exchange in single crystals for Integrated optics and optoelectronics*, Cambridge international science Publishing (1999).
- [9] J. L. Jackel, C. E. Rice, J. J. Veselka, *Appl. Phys. Lett.* **41**, 607 (1982).
- [10] K. K. Wong, *GEC. J. Res* **3**, 243 (1985).
- [11] H. Sasaki, N. Mikoshiba, *Electron. Lett.* **17**, 136 (1981).
- [12] T. D. Ni, D. Sturzebecher, M. Cummings, B. Perlman, *Appl. Phys. Lett.* **67**(12), 1651 (1995).
- [13] H. B. Lin, R. S. Cheng, W. S. Wang, *IEEE Photon. Technol. Lett.* **6**, 825 (1994).
- [14] G. Singh, A. K. Sirohi, S. Verma, *Physics of Wave Phenomena* **21**(3), 201 (2013).
- [15] R. Wigajatri Purnamaningsih, N. Raden Poespawati, E. Dogeche, D. Pavlidis, *International Journal of Technology* **4**, 701 (2016).
- [16] C. P. Vardhani, S. Neelima, *International Journal of Current Engineering and Technology* **3**(4), 1293 (2013).
- [17] L. Sirleto, M. Iodice, F. G. Della Corte, I. Rendina, *Opt. Lasers Eng.* **45**, 458 (2007).
- [18] R. Krahenbuhl, M. M. Howerton, J. Dubinger, A. S. Greenblatt, *J. Lightwave Tech.* **20**(1), 92 (2002).
- [19] E. Y. B. Pun, K. K. Loi, P. S. Chung, *Proc. SPIE, Integrated Optical Circuits* **1583**, 64 (1991).
- [20] K. K. Wong, *Proc. Soc. Photo-Opt. Instrum. Eng.*, **993**, 13 (1988).
- [21] J. Nikolopoulos G. L. Yip, *Proc. Soc. Photo-Opt. Instrum. Eng.* **1374**, 04, (1990).
- [22] J. Nikolopoulos, G. L. Yip, *J. Light. Technol.* **9**, 864 (1991).
- [23] H. Wei, J. Yu, Z. Liu, X. Zhang, W. Shi, C. Fang, *IEEE Photonics Technology Letters* **13**(5), 466 (2001).

*Corresponding author: m_kavosh@mut-es.ac.ir